

This article was downloaded by:

On: 16 January 2011

Access details: *Access Details: Free Access*

Publisher *Taylor & Francis*

Informa Ltd Registered in England and Wales Registered Number: 1072954 Registered office: Mortimer House, 37-41 Mortimer Street, London W1T 3JH, UK



## Journal of Energetic Materials

Publication details, including instructions for authors and subscription information:

<http://www.informaworld.com/smpp/title~content=t713770432>

### Synthesis and thermal properties of 1,3-dinitro-3-(1',3'-dinitroazetid-3'-yl)azetidine (TNDAZ) and its admixtures with 1,3,3-trinitroazetidine (TNAZ)

Robert L. McKenney Jr.<sup>a</sup>; Thomas G. Floyd<sup>a</sup>; William E. Stevens<sup>a</sup>; Thomas G. Archibald<sup>b</sup>; Alan P. Marchand<sup>c</sup>; G. V. M. Sharma<sup>cd</sup>; Simon G. Bott<sup>c</sup>

<sup>a</sup> Wright Laboratory, Armament Directorate, Energetic Materials Branch, Eglin AFB, FL <sup>b</sup> Aerojet, Propulsion Division, Sacramento, CA <sup>c</sup> Department of Chemistry, University of North Texas, Denton, TX <sup>d</sup> Visiting Scientist, on sabbatical leave from The Indian Institute of Chemical Technology, Hyderabad, A. P., India

**To cite this Article** McKenney Jr., Robert L. , Floyd, Thomas G. , Stevens, William E. , Archibald, Thomas G. , Marchand, Alan P. , Sharma, G. V. M. and Bott, Simon G.(1998) 'Synthesis and thermal properties of 1,3-dinitro-3-(1',3'-dinitroazetid-3'-yl)azetidine (TNDAZ) and its admixtures with 1,3,3-trinitroazetidine (TNAZ)', *Journal of Energetic Materials*, 16: 1, 1 – 22

**To link to this Article:** DOI: 10.1080/07370659808216090

**URL:** <http://dx.doi.org/10.1080/07370659808216090>

PLEASE SCROLL DOWN FOR ARTICLE

Full terms and conditions of use: <http://www.informaworld.com/terms-and-conditions-of-access.pdf>

This article may be used for research, teaching and private study purposes. Any substantial or systematic reproduction, re-distribution, re-selling, loan or sub-licensing, systematic supply or distribution in any form to anyone is expressly forbidden.

The publisher does not give any warranty express or implied or make any representation that the contents will be complete or accurate or up to date. The accuracy of any instructions, formulae and drug doses should be independently verified with primary sources. The publisher shall not be liable for any loss, actions, claims, proceedings, demand or costs or damages whatsoever or howsoever caused arising directly or indirectly in connection with or arising out of the use of this material.

# SYNTHESIS AND THERMAL PROPERTIES OF 1,3-DINITRO-3-(1',3'-DINITROAZETIDIN-3'-YL)AZETIDINE (TNDAZ) AND ITS ADMIXTURES WITH 1,3,3-TRINITROAZETIDINE (TNAZ)

Robert L. McKenney, Jr.\*, Thomas G. Floyd and William E. Stevens

Wright Laboratory, Armament Directorate, Energetic Materials Branch, Eglin AFB, FL 32542-5910

Thomas G. Archibald\*

Aerojet, Propulsion Division, P. O. Box 13222, Sacramento, CA 95813-6000

Alan P. Marchand\*, G. V. M. Sharma† and Simon G. Bott

Department of Chemistry, University of North Texas, Denton, TX 76203-0068

† Visiting Scientist, on sabbatical leave from The Indian Institute of Chemical Technology,  
Hyderabad-500007, A. P., India.

## ABSTRACT

The synthesis of TNDAZ in four steps by starting with *N*-*t*-butyl-3-hydroxymethyl-3-nitroazetidine is described. The structures of TNDAZ and of a precursor, *N*-*t*-butyl-3-nitro-3-(*N*-*t*-butyl-3'-nitroazetidin-3'-yl)azetidine, have been established unequivocally via application of single crystal X-ray crystallographic techniques. Thermal properties of TNDAZ, TNAZ and admixtures thereof are presented. A binary phase diagram has been predicted computationally and confirmed experimentally by using differential scanning calorimetry and hot stage microscopy. The thermal data support the existence of more than one polymorph for TNDAZ and for TNAZ.

## INTRODUCTION

### 1. Background

1,3,3-Trinitroazetidine (TNAZ), a novel energetic material that is of considerable interest to the Department of Defense, was first prepared by Archibald and co-workers in 1990<sup>1</sup>. In recent years, several research groups have turned their attention to developing improved methods for the synthesis of TNAZ<sup>2-5</sup>. Although TNAZ is a powerful and thermally stable energetic material, its application to melt cast explosive formulations has been limited by its high volatility characteristics and its tendency to form low density castings at atmospheric pressure<sup>6</sup>. The porosity resulting from the casting process by using pure TNAZ appears to be evenly distributed throughout the charge.

In an attempt to alter these unacceptable characteristics, researchers are endeavoring to form binary eutectic compositions with a variety of other energetic materials<sup>7</sup>. The work presented in this paper describes the synthesis and thermal characterization of 1,3-dinitro-3-(1',3'-dinitroazetidin-3'-yl)azetidine (TNDAZ) and its admixtures with TNAZ. It was anticipated that this structurally similar, yet less

Journal of Energetic Materials Vol. 16, 001-022 (1998)  
Published in 1998 by Dowden, Brodman & Devine, Inc.

volatile, material might form a binary eutectic with TNAZ that could result in a composite explosive of overall reduced volatility and of acceptable charge quality and performance.

## EXPERIMENTAL

### 1. Structural Characterization

#### a. X-ray Structures of TNDAZ and *N-t*-Butyl-3-nitro-3-(*N-t*-butyl-3'-nitroazetidin-3'-yl)azetidine (4) 8a

Data were collected on an Enraf-Nonius CAD-4 diffractometer by using the  $\omega$ -2 $\theta$  scan technique, Mo K radiation ( $\lambda = 0.71073 \text{ \AA}$ ) and a graphite monochromator. Standard procedures in our laboratory that have been described previously were used for this purpose<sup>8b</sup>. Pertinent details are presented in Table 1. Data were corrected for Lorentz and polarization effects but not for absorption. The structures were solved by direct methods (TNDAZ by MULTAN<sup>9</sup> and 4 by SHELXS86<sup>10</sup>), and the model was refined by using full-matrix least-squares techniques. The number of atoms treated with anisotropic thermal parameters depended upon the number of observed reflections. For TNDAZ, sufficient data were available to refine every non-hydrogen atom in this fashion. However, for 4, all atoms were refined as isotropic. Hydrogen atoms were located on difference maps and then included in the model as found for TNDAZ and in idealized positions [ $U(H) = 1.3 \text{ Beq(C)}$ ] for 4. All computations other than those specified were performed by using *MoIEN*<sup>11</sup>. Scattering factors were taken from the usual sources<sup>11</sup>.

### 2. Thermal Characterization

#### a. Differential Scanning Calorimetry (DSC)

Neat components, TNAZ and TNDAZ, and twenty-one TNAZ/TNDAZ mixtures were thermally characterized by using a TA Instruments, Dual Differential Scanning Calorimeter, Model 912, which was equipped with a 2100 Thermal Analyzer Data System. TA Instruments standard aluminum sample pans, Part No. 072492, were used for all melting operations. Lids, Part No. 073191, were inverted to eliminate/minimize free volume over the sample. To minimize the probability of component interaction in the mixtures and/or leakage from the sealed pans, an upper temperature limit of 105 C was enforced, as well as a sample weight limitation of 1-2 mg. A minimum of three melting/cooling operations were carried out for all samples by using a heating rate of 5 C/min. Mixtures were prepared by grinding weighed portions of dry TNAZ and TNDAZ in an agate mortar with a glass pestle to ensure homogeneity. The instrument was calibrated by using indium metal as a temperature standard. All melting points are uncorrected.

#### b. Hot Stage Microscopy (HSM)

HSM experiments were carried out by using a Mettler hot stage, Model FP 82, equipped with an FP 80 Central Processor. All observations were made with a Leitz Orthoplan Universal Largefield microscope equipped with a polarizing condenser and either a Polaroid PM-CP 3.25 x 4.25 camera or a high-resolution video system, Javelin Smart Camera, Model JE3762DSP, which was operated at shutter speeds of 1/60 and 1/500 s. The lower-power photomicrographs were obtained through a Leitz NPL 10X 0.20P lens (150x) and those at higher power through a Leitz 170/0.17 NPL Fluotar 16/0.45 lens (240x).

## RESULTS

## 1. Synthesis

### a. *N*-*t*-Butyl-3-bromo-3-nitroazetidide (2)

To a stirred solution of NaOH (2.52 g, 63 mmol) in water (25 mL), was added portionwise *N*-*t*-Butyl-3-hydroxymethyl-3-nitroazetidide (1)<sup>3</sup> (5.64 g, 30 mmol), and the resulting mixture was allowed to stir at room temperature for 3 h. The reaction mixture then was cooled via external application of an ice-water bath, and bromine (1.6 mL, 31 mmol) was added dropwise with stirring. The reaction mixture was stirred for 1 h after all of the bromine had been added. The resulting mixture was filtered, and the residue was washed with water (100 mL). The residue was dissolved in CH<sub>2</sub>Cl<sub>2</sub> (50 mL), and the resulting solution was washed successively with water (2 x 25 mL), 15 percent aqueous Na<sub>2</sub>S<sub>2</sub>O<sub>3</sub> (2 x 25 mL), and water (25 mL). The organic layer was dried (Na<sub>2</sub>SO<sub>4</sub>) and filtered, and the filtrate was concentrated *in vacuo*. The residue thereby obtained was purified via column chromatography on silica gel by eluting with 1:5 EtOAc-ligroin. Pure 2 (2.27 g, 32 percent) was thereby obtained as a pale yellow microcrystalline solid: mp 85-86 C; IR 2982 (w), 2968 (m), 2772 (s), 2555 (s), 1543 (m), 1352 (m), 1217 (m), 1125 (w), 853 (w); <sup>1</sup>H NMR (CDCl<sub>3</sub>) 0.95 (s, 9 H), 3.78 (AB, JAB = 11.0 Hz, 2 H), 4.15 (AB, JAB = 11.0 Hz, 2 H); <sup>13</sup>C NMR (CDCl<sub>3</sub>) 24.45 (q), 52.96 (s), 61.77 (t), 76.64 (s). Anal Calcd for C<sub>7</sub>H<sub>13</sub>BrN<sub>2</sub>O<sub>2</sub>: C, 35.46; H, 5.52. Found: C, 35.50; H, 5.68.

### b. *N*-*t*-Butyl-3-nitroazetidide (3)

To a solution of 2 (5.0 g, 21 mmol) in EtOH (180 mL) under nitrogen atmosphere at room temperature was added dropwise a solution of NaBH<sub>4</sub> (3.36 g, 88 mmol) in 60 % aqueous EtOH (90 mL). The resulting mixture was stirred at ambient temperature for 5 h and then was concentrated *in vacuo*. Water (60 mL) was added to the residue, and the resulting aqueous suspension was extracted with CH<sub>2</sub>Cl<sub>2</sub> (3 x 40 mL). The organic layer was washed successively with water (3 x 50 mL) and brine (25 mL), dried (Na<sub>2</sub>SO<sub>4</sub>), and filtered, and the filtrate was concentrated *in vacuo*. The residue thereby obtained was purified via column chromatography on silica gel by eluting with 1:3 EtOAc-ligroin. Pure 3 (2.65 g, 80 percent) was thereby obtained as a pale yellow oil: bp 72-74 C (0.4 mm Hg) [lit. 1 bp 50-52 C (0.1 mm Hg)]; IR 2970 (s), 2879 (w), 1547 (s), 1471 (w), 1361 (s), 1273 (w), 1234 (m), 1085 (s); <sup>1</sup>H NMR (CDCl<sub>3</sub>) 0.98 (s, 9 H), 3.66 (m, 4 H), 4.99 (m, 1 H); <sup>13</sup>C NMR (CDCl<sub>3</sub>) 24.67 (q), 51.60 (t), 52.43 (s), 71.57 (s).

### c. *N*-*t*-Butyl-3-nitro-3-(*N'*-*t*-butyl-3'-nitroazetidid-3'-yl)azetidide (4)

To a solution of KO<sup>t</sup>-Bu (2.55 g, 22.8 mmol) in EtOH (100 mL) under nitrogen was added a solution of 3 (3.00 g, 19.0 mmol) in EtOH (5 mL), and the resulting mixture was allowed to stir at room temperature for 3 h. Compound 2 (4.50 g, 19.0 mmol) then was added, and the resulting mixture was allowed to stir at ambient temperature for 48 h. The reaction mixture was concentrated *in vacuo*. Water (60 mL) was added to the residue, and the resulting aqueous suspension was extracted with CH<sub>2</sub>Cl<sub>2</sub> (3 x 40 mL). The organic layer was washed with water (2 x 50 mL), dried (Na<sub>2</sub>SO<sub>4</sub>), and filtered, and the filtrate was concentrated *in vacuo*.

To a solution of the residue thereby obtained (6.0 g) in EtOH (80 mL) at room temperature under

nitrogen was added dropwise a solution of  $\text{NaBH}_4$  (1.20 g, 31.7 mmol) in 60 percent aqueous EtOH (40 mL), and the resulting mixture was stirred at room temperature for 5 h. The reaction mixture then was concentrated *in vacuo*. Water (60 mL) was added to the residue, and the resulting aqueous suspension was extracted with  $\text{CH}_2\text{Cl}_2$  (3 x 40 mL). The organic layer was washed with water (2 x 25 mL), dried ( $\text{Na}_2\text{SO}_4$ ), and filtered, and the filtrate was concentrated *in vacuo*. The residue thereby obtained was purified via column chromatography on silica gel by eluting with 1:5 EtOAc-ligroin. This procedure afforded pure 4 (1.16 g, 19 percent) as a slightly yellowish microcrystalline solid: mp 117-118 C; IR 2975 (m), 2884 (w), 1546 (s), 1481 (m), 1363 (m), 1233 (m), 1017 (w);  $^1\text{H}$  NMR ( $\text{CDCl}_3$ ) 1.05 (s, 9 H), 3.9 (AB, J<sub>AB</sub> = 9.0 Hz, 2 H);  $^{13}\text{C}$  NMR ( $\text{CDCl}_3$ ) 24.57 (q), 52.76 (s), 54.18 (t), 83.71 (s). Anal. Calcd for  $\text{C}_{14}\text{H}_{26}\text{N}_4\text{O}_4$ : C, 53.49; H, 8.34. Found: C, 53.60; H, 8.24. The structure of 4 was established unequivocally via application of X-ray crystallographic techniques (*vide infra*).

Continued elution of the chromatography column afforded a second fraction which contained recovered 4 (2.5 g, 83 percent). The IR,  $^1\text{H}$  NMR, and  $^{13}\text{C}$  NMR spectra of the compound thereby obtained were identical in all respects with the corresponding spectra of authentic 4<sup>1</sup> (*vide supra*).

#### d. 1,3-Dinitro-3-(1',3'-dinitroazetididin-3'-yl)azetidine (TNDAZ)

A solution of 4 (1.17 g, 3.73 mmol) in fuming  $\text{HNO}_3$  (40 mL) was prepared, and the resulting solution was refluxed for 40 h. [CAUTION.- *When preparing a solution of 4 in fuming  $\text{HNO}_3$ , care should be taken to add the solid dimer in small portions with stirring to fuming nitric acid. Inverse addition of reagents may result in fire and/or explosion.*] The reaction mixture was allowed to cool gradually to ambient temperature and then was poured slowly with stirring into ice-water (60 mL), whereupon a colorless precipitate was formed. The precipitate was collected by suction filtration and was washed with cold water until the washings became neutral to litmus (150 mL). The resulting solid material was air-dried, thereby affording TNDAZ (830 mg, 77 percent) as a colorless microcrystalline solid: mp 171-173 C (dec.). Analytically pure TNDAZ was obtained by recrystallizing this material from EtOAc-ligroin as colorless platelets: mp 171-172 C (dec.); IR 3032 (w), 3011 (w), 2976 (w), 2960 (w), 2907 (vw, br), 1586 (s), 1576 (s), 1566(s), 1549 (s), 1468 (w), 1459 (w), 1441 (m), 1362 (s), 1335 (s), 1281 (s), 1192 (m), 1179 (m), 1159 (w), 1107 (w), 1018 (w), 942 (vw), 920 (w), 868 (w), 855 (w), 821 (vw), 762 (m), 604 (w), 556 (w);  $^1\text{H}$  NMR ( $\text{CDCl}_3$ ) 4.8 (AB, J<sub>AB</sub> = 15.0 Hz, 2 H), 5.05 (AB, J<sub>AB</sub> = 15.0 Hz, 2 H);  $^{13}\text{C}$  NMR ( $\text{CDCl}_3$ ) delta 62.73 (t), 80.44 (s). Anal. Calcd for  $\text{C}_6\text{H}_8\text{N}_6\text{O}_8$ : C, 24.67; H, 2.76. Found: C, 24.80; H, 2.63.

## 2. STRUCTURAL CHARACTERIZATION

Pertinent details regarding the X-ray characterization of TNDAZ are presented in Table 1. The X-ray crystal structure shows the solvent-recrystallized molecule to be oriented in a "boat" configuration with respect to the two adjacent rings.

## 3. THERMAL CHARACTERIZATION

### a. Thermal Properties of Neat TNDAZ

Individual crystals of solvent-recrystallized TNDAZ, heated at 5 C/min in the hot stage microscope,

underwent an apparent solid-solid transition at 170.8 C just prior to melting at 171.2-171.5 C. The melting range for a large sample of crystals is 170.1-172.3 C with no solid-solid transition apparent prior to melting, presumably due to the opacity of the sample. The pre- and post-transition polymorphs are hereinafter designated TNDAZ (I) and TNDAZ(II), respectively.

Thin crystalline films of TNDAZ, applied to a microscope slide with coverplate and crystallized from the melt by both crash-cooling (~140 C/min) and programmed cooling (5 C/min), exhibit a dendritic structure characterized by multi-polarization colors generally which emanate from a point source. While the crystal habit of a TNDAZ thin film does not appear to be influenced greatly by the cooling process, the effect on shrinkage crack size and pattern is significant. Specifically, crash-cooled TNDAZ is characterized by macro-shrinkage cracks that produce irregularly-shaped sections, within which are micro-shrinkage cracks which occupy primarily a concentric ring pattern (Figure 1). Program-cooled TNDAZ, on the other hand, is characterized by micro-shrinkage cracks located perpendicular to the dendritic structure. In addition, there is evidence of limited thermal decomposition in the form of gas bubble remnants.

Heating a crash-cooled TNDAZ thin film at 5 °C/min caused the polarization color pattern to change in the 110-115 C temperature range but did not affect the shrinkage crack pattern (Figure 2). This change is attributed to an annealing process that relieves

))

| Property                     | TNDAZ                | 4                   |
|------------------------------|----------------------|---------------------|
| Formula                      | $C_{14}H_{26}N_4O_4$ | $C_6H_8N_6O_8$      |
| Size (mm)                    | 0.31 x 0.35 x 0.42   | 0.04 x 0.21 x 0.23  |
| Space Group                  | C2/c                 | P21/c               |
| a (Å)                        | 17.092 <sup>1</sup>  | 15.154 <sup>2</sup> |
| b (Å)                        | 10.8654 <sup>6</sup> | 11.513 <sup>1</sup> |
| c (Å)                        | 10.640 <sup>1</sup>  | 12.903 <sup>1</sup> |
| alpha (deg)                  | 90                   | 90                  |
| beta (deg)                   | 120.910 <sup>7</sup> | 93.316 <sup>9</sup> |
| gamma (deg)                  | 90                   | 90                  |
| V (Å <sup>3</sup> )          | 1695.3 <sup>3</sup>  | 2247.4 <sup>4</sup> |
| Z                            | 4                    | 8                   |
| Dc (g-cm <sup>-3</sup> )     | 1.232                | 1.727               |
| mu (cm <sup>-1</sup> )       | 1.23                 | 1.51                |
| (2 Theta max)                | 50                   | 40                  |
| Total refl.                  | 1618                 | 2338                |
| Unique refl.                 | 1571                 | 2241                |
| R <sub>int</sub>             | 0.035                | 0.031               |
| I > 3 sigma (I)              | 1040                 | 616                 |
| Parameters                   | 100                  | 161                 |
| R, wR                        | 0.0527, 0.0479       | 0.0597, 0.0627      |
| (delta/sigma) <sub>max</sub> | <0.01                | <0.01               |
| rho min; rho max             | 0.19, -0.18          | 0.29, -0.26         |

Table 1. X-ray structure data for TNDAZ and 4.

lattice strain induced by crash-cooling. Continued heating produced still another polarization color change at 158.5 C that is believed to be associated with the solid-solid (polymorph) transition from TNDAZ (I) to TNDAZ(II). Subsequent experiments showed that this transition always occurred between 151-162 C. The color change progressed (isothermal) as paintbrush-like purple strokes which moved from left to right across the lower four-fifths of the field of view (Figure 3) and then in an upward

direction as a linear front until completion. The basic underlying shrinkage crack structure remained unchanged. A similar sample, heated at 5 C/min through the 151-162 C temperature range without a hold, resulted in only partial conversion from TNDAZ I to TNDAZ II and in melting temperatures for both polymorphs at 170.1-171.6 and 171.3-172.2 C, respectively.

DSC melting operations carried out with (a) solvent-recrystallized TNDAZ (I), (b) crash-cooled TNDAZ (I), and (c) TNDAZ (II) yielded melting temperature ranges (onset/peak) as follows: (a) 170.9/172.1, (b) 172.0/173.4, and (c) 172.1/173.0 C. The range for (a) is consistent with that from the HSM operation with (a), but is distinctly different from that of (b) and (c). The similarity of the latter two values suggests that the solid-solid transition from TNDAZ (I) to (II) in sample (b) was completed prior to melting. The heat of fusion for (a) is 6.099 kcal/mol. TNDAZ exothermically decomposed at 241/256 C (onset/peak) with an associated energy of 187 kcal/mol.

HSM cooling operations carried out at 5 C/min with liquid TNDAZ yielded crystallizations at 127.8 and 150.1 C. The first crystallization was followed by a solid-solid transition at 127.6 C, while the latter yielded only a single event. An exothermic doublet observed at 122-124 C during a DSC cooling operation is consistent with the double crystallization event at the lower temperature. The crystallization front associated with the lower temperature liquid-solid transition was continuous and irregular (Figure 4), while that for the single crystallization event resembled flattened rods (Figure 5). Neither of the final products from the above cooling operations underwent surface texture changes or darkening prior to melting in the temperature range 170.7-172.6 C.

HSM cooling experiments at a rate of approximately 70 C/min yielded only single event crystallizations in the range 109 and 102.4 C. The crystallization fronts were continuous and irregular, similar to that observed from the lower temperature event at 5 C/min. Both of these thin films underwent significant surface texture roughening with associated darkening over the temperature range 155-170 C prior to melting at 171.0-171.8 (5 C/min). In addition, a small area of the thin film that crystallized at 109 C underwent a change at 111.6 C, which is within the temperature range for the annealing process associated with the change from TNDAZ (I) strained to TNDAZ (I) annealed. While the surface texture roughening/darkening may be associated with the solid-solid transition to TNDAZ (II), the observed melting point suggests the primary component of these two thin crystalline films is TNDAZ (I) annealed. The lack of surface texture change prior to melting, as well as the shape of the crystallization fronts from the liquid state and the melting points, suggests that the final products from the cooling operations described in the previous paragraph are TNDAZ (II) with the initial product from the lower temperature event being TNDAZ (I).

#### b. Thermal Characterization of TNAZ

Thin crystalline films of TNAZ were melted (99.0-100.7 C), held at 109 C for at least two minutes, and then cooled at rates of 5 and of approximately 30 C/min. All liquids underwent spontaneous double crystallizations in the temperature range 46-61 C. The structure of the initial crystallization product is dendritic with a loosely-compacted appearance, while that of the transition product, also dendritic, possessed a very compact appearance with characteristic macro-shrinkage cracks. The latter are formed spontaneously behind the transition front as it progresses across the initial solid (Figure 6). This recrystallization characteristic, i.e., apparent compactness with associated, spontaneously-formed macro-shrinkage cracks, suggests that the density of the stable TNAZ is greater than that of the initial, unstable TNAZ. The stable TNAZ is hereinafter designated TNAZ (I) and the unstable TNAZ (II).

DSC operations at a heating rate of 5 C/min with solvent-recrystallized TNAZ afforded a sharp melting



event at 99.3/101.1 C (onset/peak) with an associated heat of fusion of 6.405 kcal/mol. TNAZ decomposed exothermically at 244/256 C (onset/peak) with an associated energy of 107 kcal/mol.

### c. Phase Diagram

The eutectic composition and melting temperature for the two component system TNDAZ/TNAZ was calculated by using a computer program <sup>12</sup> in BASIC. The program iteratively solves equation (1) (below) by using heats of fusion and melting points from both components as input data,

$$R \ln x = \Delta H_{\text{fus}} (-1/T + 1/T_0) \quad (1)$$

In equation (1), T is the melting point (degrees K) of the eutectic composition, T<sub>0</sub>, H<sub>fus</sub> and x are the melting point, heat of fusion and mole fraction of component A or B, respectively, and R is the gas constant (1.987 calories degree K<sup>-1</sup> mol<sup>-1</sup>). The calculated melting point and mol-percentage value for the TNAZ component in the eutectic composition are 90.9 C and 78.5 mol-percent, respectively. While the BASIC program <sup>12</sup> provides a graphical presentation of the phase diagram, a corresponding list of associated temperatures for the melting of each component into the eutectic composition is not provided. These temperatures were obtained by solving equation 1 for each component at selected mol fraction values.

### d. DSC Characterization of TNAZ/TNDAZ mixtures

The first heating operations for twenty-one freshly ground TNAZ/TNDAZ mixtures afforded a consistent, endothermic event at an average temperature of 90.7 +/- 0.1 C that is caused by eutectic melting. The mixtures which contain >78.5 mol-percent TNAZ also yielded a second endothermic event that is attributed to the dissolution of the TNAZ component into the liquid eutectic composition.

Re-measurements of these endothermic events with samples obtained by freezing the initial melts resulted in a shift of the eutectic endothermic events to an average temperature of 87.5 +/- 0.1 C. The eutectics from the initial and subsequent remelting operations are hereinafter referred to as "eutectic (1)" and "eutectic (2)", respectively. Remelting operations, carried out after time delays at room temperature ranging from 8 to 20 days, showed that eutectic (2) had partially reverted to eutectic (1).

### e. HSM Characterization of TNAZ/TNDAZ Mixtures

A mixed fusion slide was prepared according to the method described in McCrone <sup>13</sup>. The edges of the coverplate in contact with the zone of mixing then were sealed with an epoxy cement to prevent encroachment of air into the eutectic melt during the cooling process, a detrimental characteristic that may ruin the slide before recrystallization occurs. The slide was program-heated from 59.5 C at 1 C/min until melting of eutectics (1) and (2) occurred in the zone of mixing over the temperature range 88.0-91.4 C. Gas bubbles observed in the melt zone are believed to result from air trapped at the liquid TNAZ/solid TNDAZ interface during the slide preparation. The resolidified zone of melting after being crash-cooled is characterized by finely granulated eutectic composition (Figure 7). Reheating at 1 C/min resulted in remelting of the zone of mixing at 87.8-88.9 C (eutectic 2).

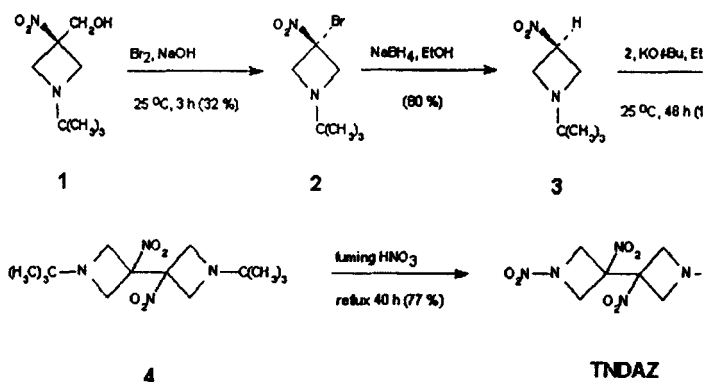
HSM heating operations with ten intimately ground mixtures of TNAZ/TNDAZ afforded melting points for the eutectic (1) and eutectic (2) compositions at average values of 90.8 and 87.9 C, respectively, and for TNAZ that were consistent with those from both DSC operations and calculations. Melting points for

the TNDAZ component were not observed during DSC operations but were obtained for two mixtures rich in TNDAZ by HSM operations. The dissolution of TNDAZ in the eutectic (1 and 2) melt is slow and requires remelting operations to affect melting of the original crystals. This resulted in inconsistent data from the TNDAZ-rich side of the eutectic composition. The characteristics of the residual crystals after the melting of eutectic (1) for mixtures around the calculated eutectic composition suggest that the TNAZ component lies between 78.0-78.8 mol-percent, a result which is consistent with the calculated value of 78.5. The calculated phase diagram along with all of the DSC- and HSM-generated data are shown in Figure 8. The unassigned data could not be related unequivocally to any particular melting event, even from HSM observations.

After initial melting operations with freshly ground TNAZ/TNDAZ mixtures followed by crash-cooling, the typically textured surface rapidly darkened upon reheating and became even more highly textured in appearance (Figure 9). This general surface darkening of the TNAZ/TNDAZ mixtures upon heating suggests that the volume of the sample is increasing vertically. This darkening results from a dimming of the underlighting as light passes through the roughened, upward-projecting, angular surface.

## DISCUSSION

The synthesis of TNDAZ is shown in Scheme 1. The starting material for this reaction sequence, i.e., 1, was prepared by using the method reported by Hiskey and Coburn<sup>4</sup>. Treatment of 1 with a solution of Br<sub>2</sub> in aqueous base resulted in retro-Henry reaction<sup>14</sup> with concomitant bromination of the resulting nitro-stabilized anion, thereby producing 2. Subsequent reaction of 2



Scheme 1

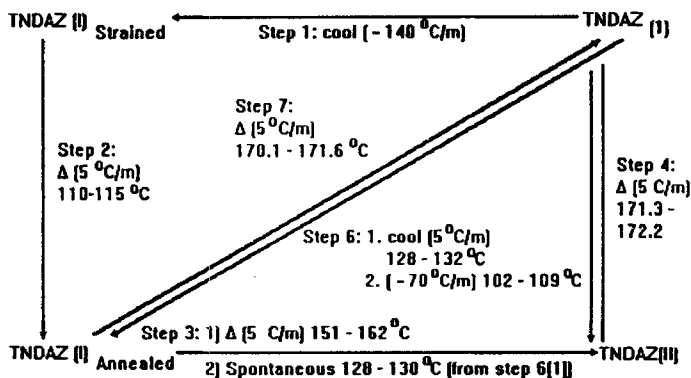
with NaBH<sub>4</sub>-EtOH resulted in selective reduction of the carbon-bromine bond in 2, thereby affording 3 in good yield. Subsequent reaction of 3 with KO<sup>t</sup>Bu-EtOH resulted in formation of the corresponding -nitro carbanion which then was reacted with 2 to form a mixture of the corresponding 3'-azetidinyl-3-azetidine (4) along with unreacted 2. In our hands, this mixture of 4 and 2 could not be separated, either by fractional recrystallization or by column chromatography. It proved advantageous to react this mixture as obtained with NaBH<sub>4</sub>. Under these conditions, 2 is reduced to 1, but 4 remains

unaffected. The resulting mixture of 4 and 1 can be separated readily via column chromatography. The structure of 4 was established unequivocally via application of X-ray crystallographic methods. Finally, when refluxed with fuming nitric acid, 4 was converted into the target molecule, TNDAZ, in good yield.

It has been demonstrated from both heating and cooling operations that TNDAZ exists in at least two polymorphic forms, (I) and (II). The sequence of conditions used to obtain these polymorphs is shown in Scheme 2.

The thin crystalline films of both polymorphs of TNDAZ are characterized by a dendritic structure with associated shrinkage cracks, the size (micro vs macro) and orientation of which are dependent on the rate of cooling. Both polymorphs are stable at ambient temperature; polymorph (II) is stable for at least 15 days. FTIR spectra (KBr) in the region  $4000\text{-}500\text{ cm}^{-1}$ , obtained from the solid TNDAZ species shown in Scheme 2 and from solvent-recrystallized TNDAZ, are similar.

TNAZ exhibits at least two polymorphic forms, (I) and (II). The unstable polymorph, (II), is observed only during the crystallization process from liquid TNAZ. It spontaneously converts to the stable form, (I), at  $30\text{ }^{\circ}\text{C}$  while simultaneously



Scheme 2

forming macro-shrinkage cracks. The change in appearance of the thin film during the transition from (II) to (I), loosely packed to compact dendritic with macro-shrinkage cracks, is consistent with a density increase and offers a logical explanation for the undesirable (highly porous) castings obtained with neat TNAZ.

It was also demonstrated that binary mixtures of TNDAZ and TNAZ result in a eutectic mixture that is influenced by polymorphism. Eutectic (1), formed from the initial melting of dry powder mixtures, undergoes transition to eutectic (2) during remelting operations. The latter exhibited limited stability at ambient temperature before reverting to (1). The experimental melting point data for the mixtures, obtained by both DSC and HSM operations, was consistent with the binary phase diagram calculated for eutectic (1) by using DSC-generated melting temperatures and heats of fusion for the individual solvent-recrystallized components.

## CONCLUSIONS

TNDAZ was prepared via a four-step synthesis route, and its structure was established unequivocally via application of single-crystal X-ray crystallographic methods. This compound was characterized thermally by using both DSC and HSM techniques, and it was found to undergo limited decomposition at its melting point.

The results of a DSC study provided melting point and heat of fusion data for TNDAZ. Thermal analysis of crystalline films by using a hot stage microscope for both heating and cooling operations provided evidence that TNDAZ exists in at least two polymorphic forms, (I) and (II).

Thermal analysis of thin crystalline films of TNAZ by using HSM cooling operations afforded evidence, in the form of double crystallizations, of polymorphism. At least two polymorphs were observed: TNAZ (I) (stable at ambient temperature) and TNAZ (II) (unstable).

Polymorphism was also exhibited by the binary mixtures of TNAZ and TNDAZ. The melting point of the initial eutectic (1) composition, obtained from the heating operation on freshly ground mixtures, decreased by 4 C for re-melting operations and thereby suggesting it had converted to eutectic (2). It was later shown that eutectic (2) slowly reverts to eutectic (1) at ambient temperature. The phase diagram for the TNAZ-TNDAZ binary system was calculated for eutectic (1) and was confirmed experimentally by DSC and HSM melting operations.

## ACKNOWLEDGMENTS

We thank the Office of Naval Research (Contract N00014-92-J-1999, to A. P. M.), the Robert A. Welch Foundation [Grants B-963 (A. P. M.) and B-1202 (S. G. B.)], the University of North Texas Faculty Research Committee (S. G. B.) for financial support of this study and to Dr. Howard H. Cady, Los Alamos National Laboratory (retired) for his unselfish discussions and sharing of expertise with regard to experimental technique and data interpretation and for his critical review of this paper.

## REFERENCES

1. Archibald, T. G.; Gilardi, R.; Baum, K.; George, C. *J. Org. Chem.* **1990**, *55*, 2920.
2. (a) Axenrod, T.; Watnick, C.; Yazdehkasti, H.; Dave, P. R. *Tetrahedron Lett.* **1993**, *34*, 6677. (b) Axenrod, T.; Watnick, C.; Yazdehkasti, H.; Dave, P. R. *J. Org. Chem.* **1995**, *60*, 1959.
3. Katritzky, A. R.; Cundy, D. J.; Chen, J. *J. Heterocyclic Chem.* **1994**, *31*, 27 1.
4. Hiskey, M. A.; Coburn, M. D. U. S. Patent 5,336,784; *Chem. Abstr.* **1994**, *121*, 300750s.
5. Marchand, A. P.; Rajagopal, D.; Bott, S. G.; Archibald, T. G. *J. Org. Chem.* **1995**, *60*, 4943.
6. Ongoing work at the Armament Directorate, Energetic Materials Branch, Eglin AFB, Florida.
7. (a) Aubert, S. A., McKenney, R. L., Jr., Sprague, C. T., Characterization of a TNAZ/PETN Composite Explosive, WL-TR-96-7012, Wright Laboratory/Armament Directorate, Eglin AFB, Florida, 30 April 1996. (b) Aubert, S. A., Sprague, C. T., Characterization of a TNAZ/TNB Composite

Explosive, WL-TR-96-7013, Wright Laboratory/Armament Directorate, Eglin AFB, Florida, 30 May 1996. (c) Aubert, S. A., Sprague, C. T., Characterization of a TNAZ/TNT Composite Explosive, WL-TR-96-7044, Wright Laboratory/Armament Directorate, Eglin AFB, Florida, 30 July 1996.

8. (a) The authors have deposited atomic coordinates for these structures with the Cambridge Crystallographic Data Center. They can be obtained, on request, from the Director, Cambridge Crystallographic Data Center, 12 Union Road, Cambridge CB2 1EZ, UK. (b) Mason, M. R.; Smith, J. M.; Bott, S. G.; Barron, A. R. *J. Am. Chem. Soc.* 1993, 115, 4971.

9. Main, P.; Fiske, S. J.; Hull, S. E.; Lessinger, L.; Germain, G.; DeClerq, J. P.; Woolfson, M. M. *MULTAN80, A System of Computer Programs for the Automatic Solution of Crystal Structures from X-ray Diffraction Data*, University of York: England; 1980.

10. *MOLEN, An Interactive Structure Solution Program*; Enraf-Nonius: Delft, The Netherlands; 1990.

11. Cromer, D. T.; Waber, J. T. *International Tables for X-ray Crystallography*; Kynoch Press: Birmingham; Vol. IV, 1974, Table 2.

12. In-house computer program written by Dr. Paul R. Bolduc.

13. McCrone, W. C., Jr., *Fusion Methods in Chemical Microscopy*, 94-101, Interscience Publishers, Inc., NY, 1957.

14. For a review of the Henry reaction, see: Baer, H. H.; Urbas, L. In: Feuer, H. (ed.) "The Chemistry of the Nitro and Nitroso Groups", Wiley-Interscience: New York, 1970, Part 2, pp 76-117.



FIGURE 1.

Thin crystalline film of **TNDZ (I)**<sub>strained</sub> (60 °C).



FIGURE 2.

Thin crystalline film of TNDZ (I)<sub>Annealed</sub>.



FIGURE 3.

Solid-solid transition from TNDAZ (I)<sub>Annealed</sub> to TNDAZ (II).





FIGURE 4.

Continuous, irregular crystal front of TNDZ (I) (127.8 °C).

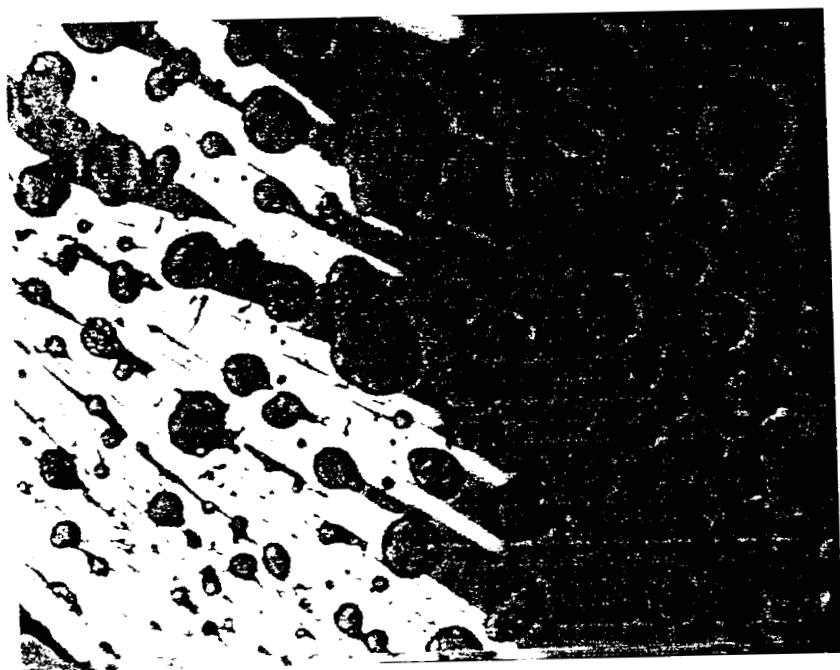


FIGURE 5.

Flattened rod crystal front of **TNDZ (II)** (150 °C).



a



b

FIGURE 6.

(a) Crystal front of **TNAZ (II)** from **TNAZ<sub>(I)</sub>**, (46 °C)

(b) thin crystalline film of **TNAZ (II)**



c



d

FIGURE 6.

(c) spontaneous transition (r to l) of TNaz (II) to TNaz (I)

(d) thin crystalline film of TNaz (I) with macro-shrinkage cracks.



FIGURE 7.

Fine-grained **TNAZ/TNDAZ** eutectic composition shown  
in the zone of mixing.

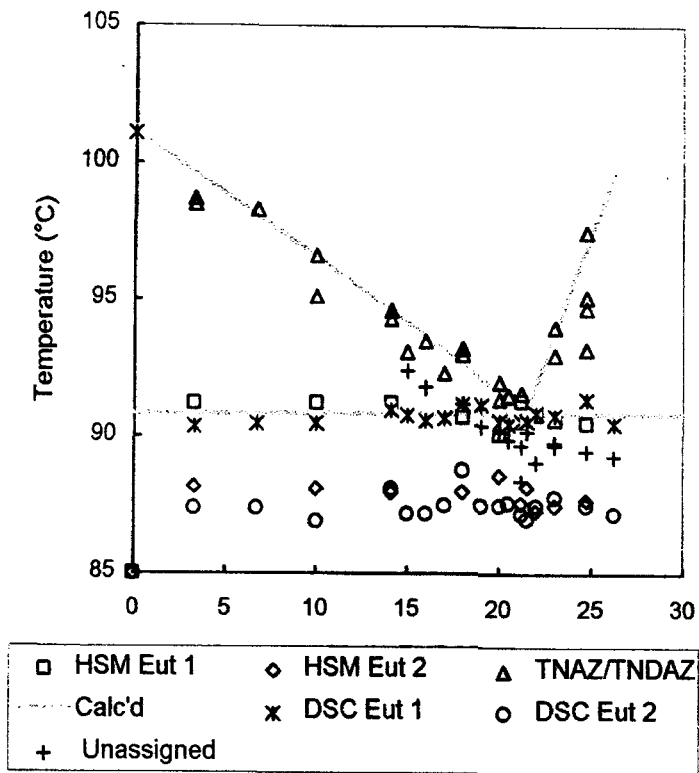


FIGURE 8.

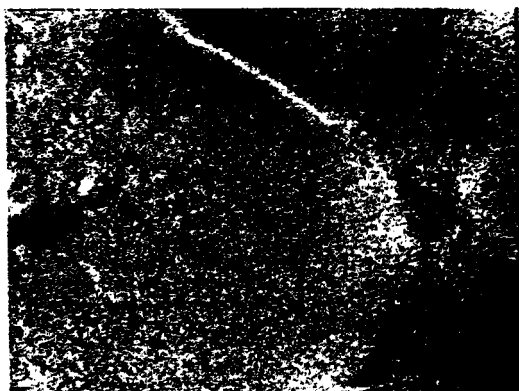
Calculated phase diagram for the TNAZ/TNDAZ system with supporting experimental data.



a



b



c

FIGURE 9. Surface texture change/darkening observed when a **TNAZ/TNDAZ** mixture containing 85.9 mol percent **TNAZ** is heated from (a) 27.0, (b) 63.0 to (c) 77.2 °C.